

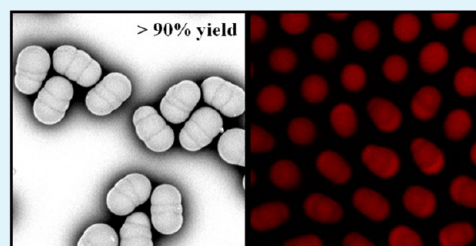
Direct Observation of the Formation of Liquid Protrusions on Polymer Colloids and their Coalescence

Bo Peng,* Alfons van Blaaderen, and Arnout Imhof*

Soft Condensed Matter, Debye Institute for NanoMaterials Science, Utrecht University, Princetonplein 5, 3584 CC, Utrecht, The Netherlands

S Supporting Information

ABSTRACT: Monodisperse nonspherical poly (methyl methacrylate) (PMMA) particles where a central core particle had grown two extra “lobes”, or protrusions, placed opposite each other were successfully synthesized by swelling and subsequent polymerization of cross-linked PMMA spheres with methyl methacrylate and the cross-linker ethylene glycol dimethacrylate. The use of large ($\sim 3 \mu\text{m}$) seed particles allowed for real-time monitoring of the swelling and deswelling of the cross-linked particles with optical microscopy. First, a large number of small droplets of swelling monomers formed simultaneously on the surface of the seed particles, and then fused together until under certain conditions two protrusions remained on opposite sides of the seed particles. The yield of such particles could be made up to 90% with a polydispersity of 7.0%. Stirring accelerated the transfer of the swelling monomers to the seed particles. Stirring was also found to induce self-assembly of the swollen seed particles into a wide variety of n -mers, consisting of a certain number, n , of swollen seed particles. The formation of these structures is guided by the minimization of the interfacial free energy between the seed particles, liquid protrusions and aqueous phase, but stirring time and geometrical factors influence it as well. By inducing polymerization the structures could be made permanent. Some control over the topology as well as overall size of the clusters was achieved by varying the stirring time before polymerization. 3D models of possible particle structures were used to identify all projections of the structures obtained by scanning electron microscopy. These models also revealed that the seed particles inside the central coalesced body were slightly compressed after polymerization. By extending the synthesis of the monodisperse particles with $n = 1$ to (slightly) different monomers and/or different cores, an important class of patchy particles could be realized.



KEYWORDS: nonspherical particles, polymer, colloid, protrusion, clusters

INTRODUCTION

Colloidal particles a few nanometers to a few micrometers in size are of great interest not only to the field of soft matter but also to that of condensed matter and materials science in general, because they can be used as ideal model systems in which they represent scaled up versions of atoms and ions, leading among other into insight into crystal nucleation and growth, the glass transition, and the influence of the range of particle–particle interactions on the phase behavior. To date, most studies of using colloids as model system focused on spherical particles or particles with simple shapes, such as rods and plates, which is mainly caused by the convenient preparation methods of these kinds of particles providing both high quantity and quality (uniform in size and shape).^{1–8} Recently, the prospect of using colloidal particles as advanced building blocks for creating functional materials has been a powerful driving force to develop new colloidal synthesis routes for colloids of more complexity and with self-assembly and functionality in mind. These more complex building blocks are expected to facilitate and expand the range of possible colloidal structures, and are promising candidates to generate new functionalities.^{9–12} Therefore, a reproducible synthesis with a high yield of nonspherical colloidal particles with a good size

distribution and shape uniformity is important, but also a huge challenge.

During the past decade, intensive efforts led to sophisticated techniques for synthesizing nonspherical colloidal particles, although some old methods already available were also rediscovered. These techniques encompass, but are certainly not limited to: arrested self-assembly by drying particles in emulsion droplets^{13–16} and seeded emulsion polymerization.^{17–36} These methods draw from the diverse fields of chemistry, physics, biology, engineering, and materials science, and, especially in combination, provide a powerful arsenal for the fabrication of new special building blocks. Among the methods mentioned, seeded emulsion polymerization received much recent attention because it is a relatively easy process, can provide for high yields, and is often reproducible. Bradford, et al.¹⁷ first described this seeded emulsion polymerization in 1962. Sheu et al.^{26,27} investigated in detail how the heating of monomer-swollen cross-linked polystyrene spheres at a few micrometer size scale caused a phase-separation of the swelling

Received: February 5, 2013

Accepted: April 17, 2013

Published: April 17, 2013

monomer (styrene) from the cross-linked seed particles in the form of a liquid protrusion which could then be polymerized. Various extensions made this technique applicable to particles of different size and with chemical and/or physical anisotropies.^{20–25,28–36} However, it is worth pointing out that most of these approaches were based on the use of cross-linked seed particles of polystyrene (PS) only and most focused on the case of a single protrusion.

The seeded emulsion polymerization method can produce more complex shapes such as linearly trimeric, cone-shaped particles, and water molecule-shaped particles by repeated swelling and polymerization,^{24,27,33} all of which are basically by variations of the swelling of seed particles followed by a phase separation.^{17–19,26,27} As mentioned, after two cycles of this procedure, linearly trimeric PS particles were usually obtained,^{24,33} but sometimes particles of other shapes appeared.²⁴ The factors that influence these differences in morphology are not well understood but addressed in the present paper, although here the focus is on trying to achieve regular particles in a single step instead of multiple. Recently, a somewhat different use of the seeded emulsion polymerization procedure was reported by Kraft et al.^{20–22} They found that cross-linked PS spheres with a liquid unpolymerized protrusion could assemble by mildly aggregating these particles into regular colloidal clusters driven by coalescence of the liquid protrusions. By controlling the amount of swelling liquid with respect to the seed particles different geometries could be obtained.²⁰ Subsequent polymerization yielded a wide variety of regular *n*-mers that ranged from clusterlike particles up to the size of colloidosomes. Here, we decided to test in more detail the mechanism generally believed to be behind the formation of the liquid protrusion which is that: the relaxation of over-swollen cross-linked seed spheres causes the extrusion of a great number of tiny liquid droplets consisting of swelling monomer; which by lowering the combined surface tension fuse into a single protrusion in the end.^{25,27,28,35}

This study resulted in a straightforward preparation of linearly trimeric particles (LTP) in one step in which not one, but two protrusions are formed on opposite sides of the micrometer-sized cross-linked poly(methyl methacrylate) (PMMA) seed particles. Particles with liquid protrusions on opposite sides of seeds, were also made by Okubo et al. and called “hamburger” particles,^{37,38} and others³⁹ in a related procedure. In this procedure, un-cross-linked polymer (mostly PS) seed particles were swollen in a polar solvent by a nonpolar solvent (e.g., alkanes) that was also a poor solvent for the PS. Under certain conditions the seed particles could be flattened between a pair of liquid protrusions by heating them at close to the glass transition temperature. In our case, an LTP is formed without a significant change in shape of the seed particle. Our method is mainly based on the seeded emulsion polymerization. Relatively large (~3 μm in diameter) cross-linked PMMA spheres are used as seeds. Direct observation (by optical microscopy) of LTP formation reveals the fusion of tiny droplets. Due to the geometry, all the small protrusions on a single seed particle merge into two primary protrusions. During the swelling process, the coalescence of PMMA seed particles with liquid protrusions upon collision, induced by stirring, is inevitable, but also results in interesting particle morphologies. The subsequent polymerization of the system can largely preserve the as-synthesized morphologies of the particles. To the best of our knowledge, this is the first time that fully PMMA complex-shaped particles are synthesized via seeded

emulsion polymerization. In addition, aided by recently developed methods, fluorescent labeling,³⁵ and transfer to apolar solvents⁴² is also possible. This makes these particles suitable for quantitative confocal microscopy studies in concentrated systems.

■ MATERIALS AND METHODS

Materials. Methyl methacrylate (MM, Aldrich) was passed over an inhibitor removal column (Aldrich) at room temperature. After the inhibitor had been removed, MM was stored in a refrigerator at +4 °C, and not longer than one month. Azo-bis-isobutyronitrile (AIBN, Janssen Chimica) was recrystallized from ethanol before use. Ethylene glycol dimethacrylate (EGDMA, Sigma) was used as the cross-linker. Polyvinylpyrrolidone (PVP, K-90, Fluka) with an average molecular weight of 360 000 g/mol was used as the stabilizer. Methanol (Biosolve, Chemical grade) was used as the solvent for dispersion polymerization. Hydroquinone (Fluka) was used as the inhibitor. (*cis*+*trans*)Decahydronaphthalene (decalin, Fluka, Chemical grade) was used as index matching solvent for PMMA. Sorbitan trioleate (Span 85, Sigma, Chemical grade) served as the phase transfer agent. The fluorescent monomers (rhodamine b isothiocyanate)-aminostyrene (RAS) was prepared following a similar method described in our previous work.⁴¹ Deionized water was used in all experiments and was obtained from a Millipore Direct-Q UV3 reverse osmosis filter apparatus.

Synthesis of Spherical Un-cross-linked Template Particles. Monodisperse spherical un-cross-linked PMMA template particles were prepared using dispersion polymerization.^{40,41} In detail, a mixture consisting of 1 g of stabilizer (PVP) and 20.5 g of solvent (methanol) was mixed with 2.5 g of monomer (MM) containing 1 wt % (based on monomer) of initiator (AIBN). The mixture was then charged into a 250 mL round-bottom flask equipped with a Teflon-coated stir bar and a condenser at room temperature. A deoxygenation process was carried out for at least 0.5 h by bubbling nitrogen through the reaction mixture. Then, the flask was immersed in a silicon oil bath at 55 °C and stirred at 100 rpm. The temperature was maintained for 24 h before cooling back to room temperature. The obtained particles were rinsed three times with methanol and two times with deionized water by using a centrifuge (Hettich Rotina 46 S centrifuge, at 315 g for 15 min), and ultimately, dispersed in a 1 wt % PVP (K-90) aqueous solution at a particle weight fraction of 0.7%. The resulting template particle radius was determined by static light scattering (SLS) to be 980 nm with a polydispersity of 2.8% (for details, see Supporting Information, Figure 1).

Synthesis of Spherical Cross-linked Seed Particles. In this step, 20 mL of template particle (0.7 wt %) aqueous suspension was charged into a round-bottom flask. In a separate container, 2 g of swelling monomer (MM) containing 2 wt % (0.04 g, based on swelling monomer) of cross-linker (EGDMA) was mixed with 1 wt % (0.02 g, based on monomer) of initiator (AIBN), and then dispersed dropwise into 20 mL of 1 wt % of PVP aqueous solution under vigorous stirring. Later, this suspension was fed dropwise (last around 5 min) into the flask containing the template particles suspension under a slow stirring (<100 rpm). Slow Feeding and stirring are critical for the formation of LTP. All samples were swollen overnight under constant stirring at 100 rpm. Subsequently, nitrogen was bubbled through the reaction system for at least 30 min to purge the system of oxygen. The addition of a water-soluble inhibitor (hydroquinone, 0.5 wt % based on swelling monomer) was to prevent secondary nucleation at an early stage of the reaction in the aqueous phase. After that, the flask was heated to 70 °C and kept at this temperature for 8 h. The suspension was then cooled to room temperature and purified by washing it four times with deionized water using a centrifuge (Hettich Rotina 46 S, at 140 g for 15 min), and finally stored in a 1 wt % PVP aqueous solution with a mass fraction of 0.7%. The obtained seed particles were monodisperse in size (1480 nm in radius and 2.5% polydispersity measured by SLS, for details, see the Supporting Information, Figure 2).

Synthesis of Nonspherical Particles. The cross-linked seed particles were used to synthesize nonspherical particles. The

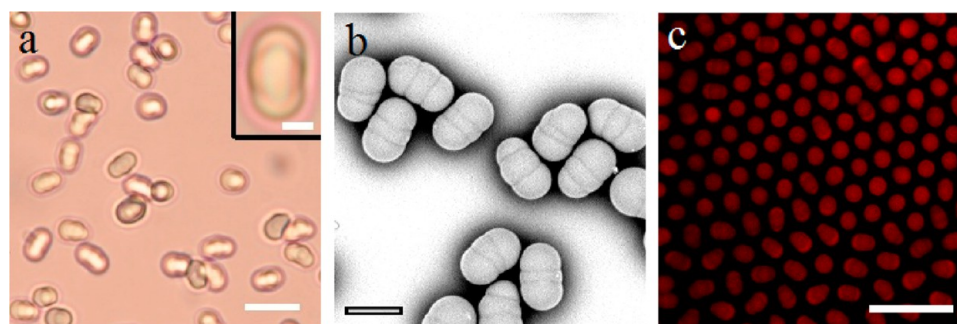


Figure 1. (a) Light microscopy image of swollen seed particles (two identical liquid protrusions are attached on the opposite sides of a seed particle); the scale bar is 10 μm and the inset one is 2 μm . (b) Scanning electron microscopy (SEM) image of typically obtained hamburger-like PMMA particles after the polymerization of liquid protrusions; the scale bar is 5 μm . (c) Confocal microscopy image of a two-dimensional plastic crystal of hamburger-like PMMA particles dispersed in a refractive index matching solvent (decalin) stabilized by Span 85 (50 mM); the scale bar is 20 μm .

preparation procedure of nonspherical particles was similar to that of the cross-linked seed particles except for the amount of swelling monomer being 4 g with 0.5 wt % (based on swelling monomer) of cross-linker (EGDMA) and 1 wt % (based on swelling monomer) of initiator (AIBN). Finally, the samples were dispersed in deionized water for characterization.

Dying Nonspherical Particles. Postdying the nonspherical particles was based on our previous work.³⁵ In brief, the suspension of nonspherical particles was first dried under a N_2 stream. The obtained dried particles (~ 0.1 g) were dispersed in a 5 mL solution of 1 mM RAS in pentanol by sonication, and stirred (~ 100 rpm) overnight in a sealed glass vial at room temperature. The labeled particles were then separated by a centrifuge (315 g, 15 min) and washed once with ethanol and twice with deionized water. After drying under a N_2 stream, the fluorescent nonspherical particles were stored in a glass vial in the dark at room temperature.

Solvent Swap. To change the solvent from high polarity to very low, we carried out a modification of the procedure developed by the Behrens group.⁴² A small amount of dried nonspherical particles (~ 0.01 g) was dispersed in deionized water and sedimented by using a Hettich Rotina 46 S centrifuge (140 g, 10 min) and the supernatant was removed. The nonspherical particles were first transferred from water to pentanol which acts as an intermediate solvent and then further to decalin containing the nonionic surfactant (Span 85, 50 mM). After this last step had been repeated four times, the solvent was considered to be completely replaced.

Characterization. To determine the size and polydispersity of the spherical particles, we performed static light scattering (SLS) on a highly dilute suspension ($\Phi < 1 \times 10^{-6}$) in deionized water with home-built equipment using a He–Ne laser as a light source (632.8 nm, 10 mW).⁴¹ The logarithm of the scattering intensity was plotted against the scattering vector $k = 4\pi n_s \sin(\theta/2)/\lambda$, where n_s is the solvent refractive index, θ is the scattering angle, and λ is the wavelength in vacuum. The SLS profiles were compared with the theoretical curves calculated with the full Mie solution for the scattering form factor for particles with a core–shell or homogeneous structure. Polydispersity was accounted for in the calculation by integrating over a Gaussian size distribution taking into account the size-dependent scattering intensity.⁴³

Taking advantage of the relatively large size (in a micrometer-sized scale) of the particles presented in this paper, the swelling behavior and the particle morphologies in preparations were easily recorded in real time with an optical microscope equipped with a 63 \times objective. These pictures were captured with a digital Nikon camera (D90), whereas the polymerized particles were examined using a scanning electron microscope (SEM, Phenom). The samples were sputter coated with 5 nm platinum prior to imaging. Confocal scanning laser microscopy (CSLM) was used to record the phase behavior of the fluorescent nonspherical particles in the absence of interference from the refractive index mismatch between solvent and particles. A Nikon confocal scanning laser scan head (Nikon C1) was operated in fluorescent mode on a Leica (DM IRB) inverted microscope. A Leica

63 \times oil confocal immersion lens with a numerical aperture of 1.4 was used for measurement. The fluorescent dye was excited at around 543 nm and the images were collected at emission wavelengths of around 605 nm.

RESULTS AND DISCUSSION

Sample Preparation. Recently, seeded emulsion polymerization techniques have been successfully employed in the fabrication of various types of anisotropic polymer particles. Typically, cross-linked polymer spheres suspended in an aqueous environment are swollen with hydrophobic monomers, such as methyl methacrylate or styrene. Upon relaxation of the stretched polymer network, the strongly swollen polymer sphere phase separates, yielding a mildly swollen polymer sphere carrying a liquid protrusion consisting of swelling monomer. This relaxation can be enhanced by temperature elevation as well as a long swelling time.^{23,26,27} The resulting particles were reported to be mainly dimers,^{23,25–32,34,35} but also popcornlike^{27,35} and, after merging of the liquid protrusions on different seed particles with a single protrusion, also colloidal molecule-like shapes were seen.^{20,21} As mentioned before, the work of Okubo et al.^{37–39} on the swelling and wetting by apolar solvents of polymer seed particles dispersed in polar liquids is closely related to the liquid protrusions. The only difference is that protrusions made from a monomer usually can be made permanent by polymerization.

Sheu et al.^{26,27} proposed that at first multiple liquid protrusions formed on highly cross-linked seed particles (PS). They supposed that this could be attributed to in-homogeneities of the network, which tend to localize contraction forces during swelling. Until now, the number and position of multiple protrusions was mostly uncontrolled and research focused on this topic is rare.^{24,26,27,35} Kraft et al. showed that by stabilizing the protrusions on PS and poly (N-isopropylacrylamide) (PNIPAM) spheres with increasing amounts of surfactant their final number can be controlled.²²

We first followed (with slight modifications, for details, see the experimental section) the procedure which was originally from Sheu's work²⁶ for preparing dumbbell-like PMMA particles instead of PS. The cross-link density of the seed particles was controlled at 2 wt % based on the mass of the monomers. The process of absorption and then the release of swelling monomers caused a phase separation between the swelling monomers and seed particles, forming liquid protrusions. Subsequently, heating induced polymerization of the monomers and also enhanced the phase separation leading to the growth of the protrusions. Surprisingly, PMMA seed

particles with two newly formed identical liquid lobes or protrusions (also called “hamburgerlike” particles by others^{37–39}) were obtained, even after polymerization of these liquid protrusions and rinsing away the impurities, the shape maintained (see Figure 1a, b). It is worth pointing out that the two new-formed lobes were always located opposite from each other on the surface of a seed particle, which is why we denote these as: linearly trimeric particles (LTP), where the “trimeric” here does not refer to the number of seeds, but to the number of separate segments visible. Note that LT structure was independent of the swelling monomer composition; it appeared even if only a pure monomer (MM) instead of a mixture of monomer and cross-linker was used. This feature demonstrates the potential that our approach could be extended to a more universal method for preparing such LT-structured polymer particles with more chemical and/or physical anisotropies. For instance, by slightly modifying the procedure in which small quantities of other monomers are used in the swelling would result in particles where the charge density on the opposite lobes would be different from that of the seed particle. From computer simulations and theory, it is clear that the self-assembly behavior of such particles is quite interesting.^{44,45} For self-assembly studies, it is quite important to be able to synthesize particles in bulk as for instance methods that rely on 2D methods will give a much lower yield of particles.⁴⁵

Plastic Crystals. Colloidal hard dumbbells were computationally predicted to form a plastic crystal at aspect ratios lower than 0.4.^{46,47} Our group recently observed such plastic crystals in soft dumbbell systems (in 2D and 3D); these plastic crystals could be switched to full crystals by virtue of an electric field.^{35,48} Drawing inspiration from Espinosa’s work,⁴² the as-synthesized LT PMMA particles were efficiently transferred from a polar (water) to nonpolar solvent (hexane or decalin) by means of a nonionic surfactant (span 85) which keeps the Debye–Hückel screening length larger than the particle size. Soft plastic crystals made of the LT particles (LTP) were observed in two dimensions as shown in Figure 1c. The orientations of the LT PMMA particles are disordered, whereas the positions are ordered. Therefore, because of the long screening length of each particle in Figure 1c, plastic crystals made of LT particles in 3D are feasible as well and will be described in a forthcoming publication.

Stirring Effect. During the swelling of seed particles, stirring was discovered to accelerate the formation of LTP, which is most likely caused by the fact that stirring speeds up the transport of monomer, which would otherwise be limited to slow molecular diffusion through the aqueous phase. As shown in images a and b in Figure 2, in the absence of stirring, swelling monomers diffused to the polymer phase much more slowly. Even after a day, there was only a small change in the morphology of the particles. On the other hand, stirring efficiently accelerated the transfer of the swelling monomers; images c and d in Figure 2 clearly demonstrate this fact.

Formation Exploration. To elucidate the formation mechanism of the LT-shaped particles, we tried imaging of swollen particles as a function of time. In order to directly observe the formation of liquid protrusions, a capillary (50 mm × 2 mm × 0.2 mm) was initially half-filled with a suspension of seed particles. It was placed in a horizontal position. After half an hour, the density difference between the seed particles and solvent (water) forced the particles to sediment to the bottom of the capillary, where they stayed roughly stationary (due to

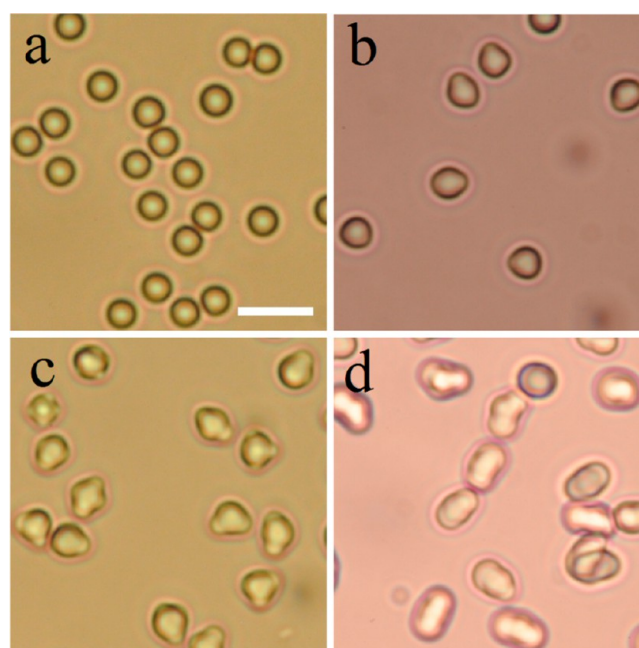


Figure 2. Optical microscopy images of swollen seed particles, without stirring at (a) ~ 30 s and (b) a day, and with stirring at (c) ~ 30 s and (d) 10 min. The scale bar is $10 \mu\text{m}$.

the big size of the particle $\sim 1.5 \mu\text{m}$ in radius). Subsequently, the emulsion containing swelling monomers stabilized by PVP was fed carefully and slowly into the remaining half of the capillary using a 1 mL syringe, so as to not significantly disturb the locations of the seed particles. The swelling monomer emulsion comprised a large number of tiny droplets of swelling monomers that were too small to visible under an optical microscope, but could be observed by light scattering. Swelling monomer in the form of these small droplets was efficiently absorbed by the seed particles. There also were big droplets of swelling monomer but due to the density difference with the swollen seed particles, these droplets floated to the top of the capillary. Therefore, it was easy to accurately observe the swelling behavior of the seed particles directly at the bottom of the capillary without too much disturbance from the big swelling monomers droplets. The summarized optical micrographs and corresponding schematic cartoons are shown in Figure 3.

Once the emulsion of swelling monomers was mixed with the seed particles dispersion, numerous small swelling monomer droplets were gradually absorbed by the seed

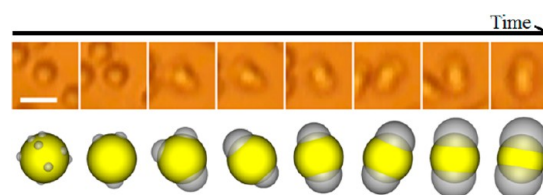


Figure 3. Time-lapse optical microscopy (top row) and corresponding schematic images (lower row) of the formation and growth of the biliquid protrusions on the surface of a cross-linked (2 wt %) PMMA seed particle. The lower row shows schematic images with the seed particles and newly formed protrusions being marked yellow and gray in color, respectively. The total time scale is about 10 min and the scale bar is $5 \mu\text{m}$.

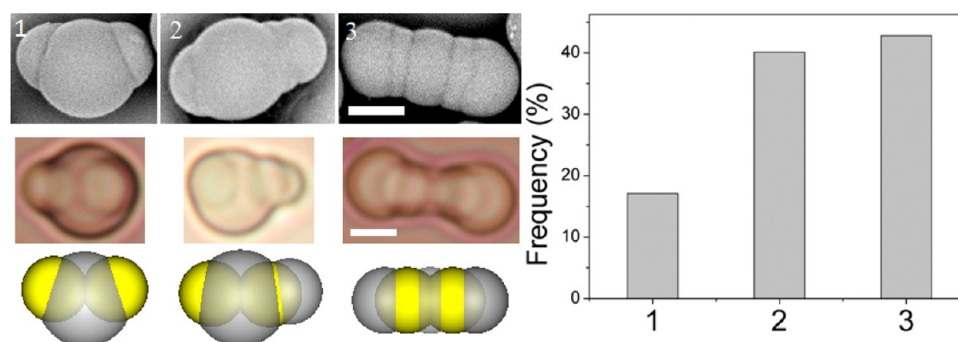


Figure 4. Colloidal PMMA clusters comprised of two seed particles, before (optical microscopy images) and after (SEM images) polymerization. Schematic representations are shown in the bottom row; the seed particles and newly formed protrusions are marked yellow and gray in color, respectively. The bar graph shows their relative abundance. The scale bars are 3 μm .

particles in which the swelling monomers swelled the cross-linked polymer network, resulting in expansion of the seed particles in the early stage of swelling. Then, shrinkage²⁷ of the cross-linked polymer network took place, leading to many tiny droplets comprised of swelling monomers to protrude out. The tiny droplets tended to fuse so as to lower their combined surface energy. As a result of the continued fusion among the small swelling droplets on the surface of a seed particle, only three primary liquid protrusions are visible in the third image in Figure 3. Two of these are located closer to each other than to the third one. When the liquid protrusions grew bigger, the two closer protrusions merged into a bigger one leaving only two (also see the movie in the Supporting Information). Interestingly, these nonidentical liquid protrusions grew to an identical size over time and did so for almost all particles (~79%, the remaining 21% were seed particles with single or multiple protrusions) at this stage. In the last optical image in Figure 3, a spherical seed particle with two identical liquid protrusions aligned linearly is presented. Polymerization afterward did not influence this LT-shaped morphology (see Figure 1). It is worth pointing out that the yield of LTP can be increased up to 90% by repeating centrifugation.

In our previous work,³⁵ small PMMA particles (around 1 μm in diameter) with the same cross-link density were used as seeds to prepare nonspherical particles via the seeded emulsion polymerization technique. During the stirring and subsequent polymerization stage, just one single protrusion was visible on each seed particle. Hence, it can be concluded that the formation of LTP is geometry (size)-dependent, because it mainly took place on the relatively large-sized seeds (e.g., 1.5 μm in radius). Kraft et al.²⁰ introduced a synthetic method for assembling colloidal spheres into clusters by making use of liquid protrusions on the surfaces of cross-linked PS seed particles. They mentioned that they never observed more than one protrusion on small seed particles (PS, 222 nm in diameter), whereas for the big seed particles (PS, 1.88 μm in diameter) sometimes secondary protrusions were found that were significantly smaller than the primary protrusions. They believed that the formation of more than one protrusion was unfavorable in terms of surface energy, and the protrusions on the surface of a seed particle coalesced over time. Clearly, for a larger surface area per particle both the chance of getting multiple protrusions and the time they take to fuse will go up. To confirm it, our swelling systems were kept stirring under gentle stirring (~100 rpm) for 5 days. As a result, seed particles with only a single liquid protrusion attached prevailed, which implies that the LTP is only a transient state, with longer

coalescence or ripening time. As expected, by refraining from stirring we noticed that once the LTP were dominant, these LT-structures were preserved for a longer time span (at least five days), giving ample time to freeze them in by polymerization. It may be that charges on the protrusions and/or a deformation of the central seed may delay the coalescence of the two opposing protrusions into one, a configuration with a lower free energy. Similar observations were also made by Kraft et al. in a later paper on protrusions made on PS and PNIPAM.²² Further research is necessary to determine the optimal conditions of the synthesis of the LTP, which were also found by Okubo et al.^{37,38} under certain conditions when they did not swell seeds with monomers, but with apolar liquids.^{37,38} But in that case, the seed particle shape was strongly changed (flattened).

Clusters. As mentioned above, stirring was crucial in our system. Without constant gentle stirring, the saturation of the cross-linked polymer network with swelling monomer took a relatively long time. Alternatively, fast stirring (faster than 100 rpm) tended to cause the swollen seed particles to flocculate in the form of the visual agglomerations. On the other hand, after the formation of LT structures on the seed surfaces had taken place, constant gentle stirring induced the self-assembly by coalescence of the liquid protrusions on different colloids.^{20–22} In principle, the more liquid droplets are present on the surface of the seed particles if they coalesce, the larger the number of combinations of colloidal structures that will be obtained. Specifically, for seeds with a single protrusion attached, all obtained colloidal structures with a given number of seed particles have an identical geometry.^{20,21} When a secondary identical liquid droplet is “added” to the surface of a seed particle, the combinatorial potential of such a colloid increases rapidly, not only because of the fusion of liquid droplets on a similar seed particle, but also that of those on different seeds. Clusters made up of two seed particles are shown in Figure 4. Already here it is clear that the structures obtained are not unique, although the small number could still possibly be purified if a suitably sensitive technique would be used.

To reveal in more detail the internal structures of the clusters obtained, we tried to overlap images of the clusters ($n = 2, 3$, where n is the number of the seed particles contained in a cluster) based on the observation of a large number of such clusters from SEM with projections of 3D models. The 3D models were constructed according to the contacting angle (θ), bond angle α (for $n = 2$), β (for $n = 3$), the radius of the seed particles (R_s), individual (R_i), and coalesced protrusions (R_c), and the distance between two seeds centers (L) (see the

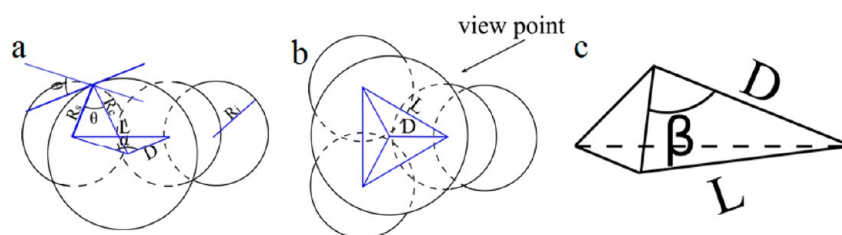


Figure 5. Schematic representations of (a) a dimeric cluster (comprising two seed particles, and corresponding to the case in Figure 4-2); (b) a trimeric cluster (comprised of three seed particles, and corresponding to the case in Figure 6-2); (c) shows the pyramid formed by centers of the seeds and the center of the coalesced protrusion. L is the distance between the centers of two seeds, θ is the contact angle, α (for clusters that comprise two seeds) and β (for clusters that comprise three seeds) are the bond angles, R_s , R_c , and R_s correspond to the radius of the seed particles, individual, and coalesced protrusions, respectively.

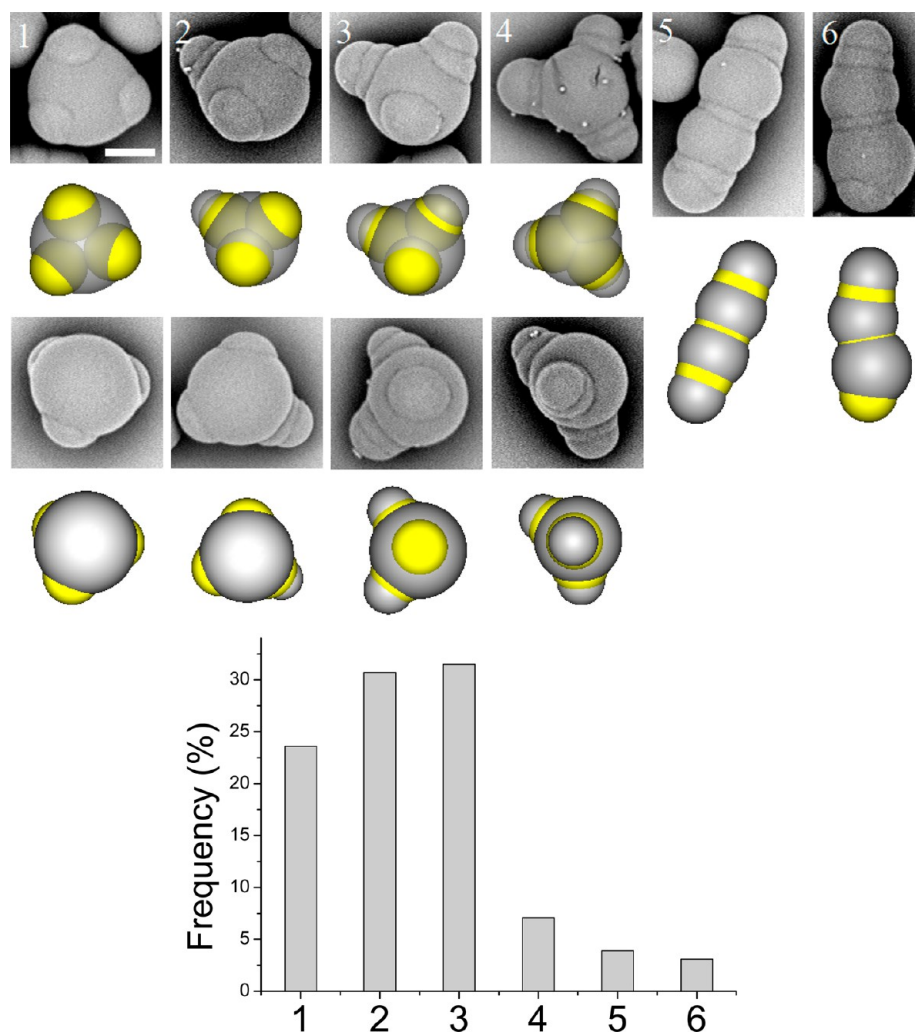


Figure 6. Colloidal PMMA clusters comprising three seed particles (SEM images) and their respective 3D model representations and relative abundance. The scale bar is $3 \mu\text{m}$.

schematic models in Figure 5) and based on an assumption in which we assumed the distances (D) from the center of coalescent protrusion to that of seed particles were identical (see Figure 5). Specifically, the bond angle α and β in a cluster can be calculated via

$$\alpha = \cos^{-1} \left(1 - \frac{L^2}{2(R_c^2 + R_s^2 - 2R_c R_s \cos \theta)} \right) \quad (1)$$

$$\beta = \cos^{-1} \left(1 - \frac{L^2}{2(R_c^2 + R_s^2 - 2R_c R_s \cos \theta)} \right) \quad (2)$$

By only rotating these models, i.e., changing the viewpoint, we could reproduce all observed colloidal clusters. Good agreement between models and experiments required that the seed particles interpenetrated slightly (i.e., $L < 2R_s$, see Figure 4). Similarly, for the trimeric clusters ($n = 3$) the seed particles partially overlapped inside the center in the coalesced protrusion body. However, the sizes of the overlap varied

with the sizes of the coalesced protrusions. The perspective images in Figure 4 clearly show, from left to right, a tendency to increase the overlap, which is mainly caused by the decrease in size of the coalesced protrusions. However, a deformation of the seed particles to conform more to the surface tension of the monomer protrusions could also partially explain these results. This would be similar to the work of Okubo et al.,^{37,38} who observed organic solvents in/onto seed particles and investigated on how these liquid deformed the spherical seeds to anisotropic shapes. The smaller the coalesced protrusion are, the more severe the interpenetration and/or deformation. This “soft” behavior can be understood by considering that the polymer network of the seeds was only cross-linked by 2% w/w cross-linker, and that the swelling monomers inherently are good solvents for their polymer. Again, the configurations of dimers were maintained after polymerization, as seen from the optical microscopy and SEM images in Figure 4. Moreover, the bond angle α increased when less liquid contributed to the coalesced central body (α are 144 and 162° for the cases in Figure 4-1 and 2, respectively). When the coalesced central body was composed of two liquid protrusion units, the two seed particles, as well as their protrusions, aligned linearly ($\alpha = 180^\circ$), which is shown in Figure 4-3. It is possible that the volume of the coalesced protrusions is too small in this case, restricting the movement of the seed particles inside the fused protrusions as was seen before in the work of Kraft et al.²¹ Additionally, the total volumes of the liquid protrusions obtained using the 3D models for each configuration was roughly equal for the clusters with a given n , namely, the total volume of liquid protrusions depended only on how many seed particles (n) were contained in the clusters.

Although the total volume of liquid protrusions for each n clusters was fixed, the coalesced protrusion size was variable, and mainly depended on the number of liquid protrusion units (the particle with only one protrusion we counted as two protrusion units) that fused to form it. For $n = 3$, six distinct combinations were found and listed in Figure 6. To not confuse with bond angle (α) in dimeric clusters ($n = 2$), we define the bond angle β for clusters (only applicable for the first four samples in Figure 6) with three seeds as the angle between the center of the coalesced (largest) protrusions and any two seed particles (for more details, see Figure 4). The bond angles in the clusters comprising three seeds show a gradual increase as the size of the coalesced droplet grows from left to right in the first four samples in Figure 6 (from 104° to 110°). This means the sizes of the centrally coalescent bodies of the clusters could be adjusted by the number of fused liquid protrusion units, and directly affects the variation of the bond angles as well. From the fact that the overlap fractions increased when fewer liquid protrusions participated in the centrally coalesced bodies, it can be inferred that the seed particles were less mobile when fewer liquid protrusion units join in before polymerization. The subsequent polymerization caused shrinkage of the newly formed central polymer body according to the density increase from liquid monomer to solid polymer network, and ultimately, resulted in a higher overlap fraction of seeds inside the central body.

Inspecting image 6 in Figure 6, one individual and two coalesced protrusions are present from the top to bottom of the cluster. The first coalesced protrusion from the top comprised of two liquid protrusion units, which is not large enough to let two attached seed particles move freely, whereas the bottom one comprised three liquid protrusion units, which indicates a

small deviation of bond angle away from linear alignment (bond angle is 162°). One can roughly deduce a critical number of protrusion units, a larger number than which would lead to a nonlinear alignment of the seeds, whereas a smaller number induces only a linear alignment of the seeds. It turns out that in our case, this critical number equals 2. This is in good accordance with the case in Figure 4-2. In image 5 of Figure 6, a linear rodlike cluster is shown consisting of three seed particles that each carries two protrusions. Both protrusions on the central seed have coalesced with one of the protrusions on another seeds. The second protrusion on each of those other seeds did not coalesce. This resulted in a linear cluster with a central seed particle (also see the corresponding 3D model representation below the sample 5 in Figure 6). As just mentioned, when the number of liquid protrusion units is 2 or less only a linear alignment of the seeds with protrusions is observed. Again, sample 5 in Figure 6 supports this rule. The lack of more than 2 liquid protrusion units in the coalesced protrusions maintains the linear alignment of seed particles. A statistical analysis of the morphologies of the clusters consisting of three seed particles was carried out based on measuring more than 200 experimental (SEM) images, and the results are shown in Figure 6. It clearly shows that the most favorable configurations of clusters ($n = 3$) are the first three cases (see Figure 6-1, 2, and 3). In comparison, clusters 5 and 6, which both exhibit a linear configuration, were rare because of their high surface energies.

In principle, the landscape of clusters undergoes an explosive increase for $n > 3$. However, in absolute number these clusters were rarely present because of the relatively short stirring period and the low stirring speed. The five typical configurations for the clusters comprising four seed particles ($n = 4$) are shown in Supporting Information, Figure 3. Because of the significantly lower number of SEM images for $n = 4$ clusters, the statistics could not be determined. However, an apparent tendency is that the size of the uncoalesced protrusions on the seed particles decreased when the number of individual protrusions increased.

CONCLUSIONS

Monodisperse PMMA particles with two opposing protrusions on the central seed particles were fabricated via a one step seeded emulsion polymerization by using 2 wt % cross-linked PMMA spheres as seeds, despite of the fact that this configuration is only metastable with respect to a single protrusion. The formation of such nonspherical particles was recorded in real time by optical microscopy. Initially, the monomer swells the seeds and then numerous tiny monomers droplets were extruded out onto the surface of the swollen seeds. Driven by the surface energy and geometry, fusion of the swelling monomers droplets took place, and finally only two primary liquid droplets were left, attached to the surface of the seed particles. At this stage, a nearly monodisperse system of linear-trimeric particles could be obtained. Such particles with opposing lobes are interesting for self-assembly studies as has already been shown in computer simulations.⁴⁴ This synthesis route provides an easier method with a significantly higher yield than for instance trimeric patchy particles made by oblique evaporations or other 2D methods.⁴⁵ Stirring enhanced further coalescence of the liquid protrusions, either between protrusions on particles of the same type or between those on different types of particles. This led to the formation of complex colloidal clusters, which were unfortunately not unique

for clusters built up from the same number of seeds. The subsequent polymerization of the liquid protrusions did not change the configurations any further. 3D modeling of the obtained clusters offered insight into the internal structures of clusters. These plentiful "isomeric" colloidal molecules are interesting candidates for materials research.

■ ASSOCIATED CONTENT

■ Supporting Information

Characterization of seed particles, the cluster of $n = 4$, and the movie of the formation of liquid protrusions. This material is available free of charge via the Internet at <http://pubs.acs.org>.

■ AUTHOR INFORMATION

Corresponding Author

*E-mail: b.peng@uu.nl (B.P.); A.Imhof@uu.nl (A.I.).

Notes

The authors declare no competing financial interest.

■ ACKNOWLEDGMENTS

Bas Kwaadgras is acknowledged for fruitful discussions. This work was funded through Nanodirect FP7-NMP-2007-SMALL-1, project 213948.

■ REFERENCES

- (1) van Blaaderen, A.; Wiltzius, P. *Science* **1995**, *270*, 1177–1179.
- (2) van Blaaderen, A. *Prog. Colloid Polym. Sci.* **1997**, *104*, 59–65.
- (3) Yetheraj, A.; van Blaaderen, A. *Nature* **2003**, *421*, 513–517.
- (4) van Megen, W.; Underwood, S. M. *Nature* **1993**, *362*, 616–618.
- (5) Leunissen, M. E.; Christova, C. G.; Hynninen, A. P.; Royall, C. P.; Campbell, A. L.; Imhof, A.; Dijkstra, M.; van Roij, R.; van Blaaderen, A. *Nature* **2005**, *437*, 235–240.
- (6) Shevchenko, E. V.; Talapin, D. V.; Kotov, N. A.; O'Brien, S.; Murray, C. B. *Nature* **2006**, *439*, 55–59.
- (7) Kuijk, A.; van Blaaderen, A.; Imhof, A. *J. Am. Chem. Soc.* **2011**, *133*, 2346–2349.
- (8) van der Beek, D.; Lekkerkerker, H. N. W. *Langmuir* **2004**, *20*, 8582–8586.
- (9) Glotzer, S. C.; Solomon, M. J. *Nat. Mater.* **2007**, *6*, 557–562.
- (10) Duguet, E.; Desert, A.; Perro, A.; Ravaine, S. *Chem. Soc. Rev.* **2011**, *40*, 941–960.
- (11) Perro, A.; Reculusa, S.; Ravaine, S.; Bourgeat-Lami, E.; Duguet, E. *J. Mater. Chem.* **2005**, *15*, 3745–3760.
- (12) Yan, S.; Kim, S.; Lim, J.; Yi, G. *J. Mater. Chem.* **2008**, *18*, 2177–2190.
- (13) Manoharan, V. N.; Elsesser, M. T.; Pine, D. J. *Science* **2003**, *301*, 483–487.
- (14) Yi, G. -R.; Manoharan, V. N.; Michel, E.; Elsesser, M. T.; Yang, S. -M.; Pine, D. J. *Adv. Mater.* **2004**, *16*, 1204–1208.
- (15) Cho, Y.-S.; Yi, G.-R.; Lim, J.-M.; Kim, S.-H.; Manoharan, V. N.; Pine, D. J.; Yang, S. -M. *J. Am. Chem. Soc.* **2005**, *127*, 15968–15975.
- (16) Cho, Y.-S.; Yi, G.-R.; Kim, S.-H.; Pine, D. J.; Yang, S.-M. *Chem. Mater.* **2005**, *17*, 5006–5013.
- (17) Bradford, E. B.; Vanderhoff, J. W. *J. Polym. Sci., Part C* **1962**, *3*, 41–46.
- (18) Okubo, M.; Katsuta, Y.; Matsumoto, T. *J. Polym. Sci., Polym. Lett. Ed.* **1980**, *18*, 481–486.
- (19) Skjeltorp, A. T.; Ugelstad, J.; Ellingsen, T. *J. Colloid Interface Sci.* **1986**, *113*, 577–582.
- (20) Kraft, D. J.; Vlug, W. S.; van Kats, C. M.; van Blaaderen, A.; Imhof, A.; Kegels, W. K. *J. Am. Chem. Soc.* **2009**, *131*, 1182–1186.
- (21) Kraft, D. J.; Groenewold, J.; Kegels, W. K. *Soft Matter* **2009**, *5*, 3823–3825.
- (22) Kraft, D. J.; Hilhorst, J.; Heinen, M. A. P.; Hoogenraad, M. J.; Luigjes, B.; Kegels, W. K. *J. Phys. Chem. B* **2011**, *115*, 7175–7181.
- (23) Kim, J. -W.; Larsen, R. J.; Weitz, D. A. *J. Am. Chem. Soc.* **2006**, *128*, 14374–14377.
- (24) Kim, J.-W.; Larsen, R. J.; Weitz, D. A. *Adv. Mater.* **2007**, *19*, 2005–2009.
- (25) Kim, J. -W.; Lee, D.; Shum, H. C.; Weitz, D. A. *Adv. Mater.* **2008**, *20*, 3239–3243.
- (26) Sheu, H. R.; El-Aasser, M. S.; Vanderhoff, J. W. *J. Polym. Sci., Part A: Polym. Chem.* **1990**, *28*, 629–651.
- (27) Sheu, H. R.; El-Aasser, M. S.; Vanderhoff, J. W. *J. Polym. Sci., Part A: Polym. Chem.* **1990**, *28*, 653–667.
- (28) Mock, E. B.; De Bruyn, H.; Hawkett, B. S.; Gilbert, R. G.; Zukoski, C. F. *Langmuir* **2006**, *22*, 4037–4043.
- (29) Mock, E. B.; Zukoski, C. F. *Langmuir* **2010**, *26*, 13747–13750.
- (30) Ge, J.; Hu, Y.; Zhang, T.; Yin, Y. *J. Am. Chem. Soc.* **2007**, *129*, 8975–8975.
- (31) Nagao, D.; Hashimoto, M.; Hayasaka, K.; Konno, M. *Macromol. Rapid Commun.* **2008**, *29*, 1484–1488.
- (32) Nagao, D.; van Kats, C. M.; Hayasaka, K.; Sugimoto, M.; Konno, M.; Imhof, A.; van Blaaderen, A. *Langmuir* **2010**, *26*, 5208–5212.
- (33) Park, J.-G.; Forster, J. D.; Dufresne, E. R. *Langmuir* **2009**, *25*, 8903–8906.
- (34) Park, J. -G.; Forster, J. D.; Dufresne, E. R. *J. Am. Chem. Soc.* **2010**, *132*, 5960–5961.
- (35) Peng, B.; Vutukuri, H. R.; van Blaaderen, A.; Imhof, A. *J. Mater. Chem.* **2012**, *22*, 21893–21900.
- (36) Kegels, W. K.; Breed, D.; Elsesser, M.; Pine, D. J. *Langmuir* **2006**, *22*, 7135–7136.
- (37) Fujibayashi, T.; Okubo, M. *Langmuir* **2007**, *23*, 7958–7962.
- (38) Fujibayashi, T.; Tanaka, T.; Minami, H.; Okubo, M. *Colloid Polym. Sci.* **2010**, *288*, 879–886.
- (39) Hosseinzadeh, S.; Saadat, Y.; Abdolbaghi, S. *Colloid Polym. Sci.* **2012**, *290*, 847–853.
- (40) Shen, S.; Sudol, E. D.; El-Aasser, M. S. *J. Polym. Sci., Part A: Polym. Chem.* **1993**, *31*, 1393–1402.
- (41) Peng, B.; van der Wee, E.; Imhof, A.; van Blaaderen, A. *Langmuir* **2012**, *28*, 6776–6785.
- (42) Espinosa, C. E.; Guo, Q.; Singh, V.; Behrens, S. H. *Langmuir* **2010**, *26*, 16941–16948.
- (43) Bohren, C. F.; Huffman, D. R.; *Absorption and Scattering of Light by Small Particles*; John Wiley and Sons: New York, 1983; Vol. 4, p 83.
- (44) Bianchi, E.; Kahl, G.; Likos, C. N. *Soft Matter* **2011**, *7*, 8313–8323.
- (45) Chen, Q.; Bae, S. C.; Granick, S. *Nature* **2011**, *469*, 381–384.
- (46) Vega, C.; Monson, P. A. *J. Chem. Phys.* **1997**, *107*, 2696–2697.
- (47) Marechal, M.; Dijkstra, M. *Phys. Rev. E* **2008**, *77*, 061405.
- (48) Demirors, A. F.; Johnson, P. M.; van Kats, C. M.; van Blaaderen, A.; Imhof, A. *Langmuir* **2010**, *26*, 14466–14477.